Determination of the surface-potential barrier of Cu(001) from low-energy-electron-diffraction fine structure

G. J. Hitchen, S. M. Thurgate, and P. J. Jennings
School of Mathematical and Physical Sciences, Murdoch University, Murdoch, 6150 Western Australia, Australia
(Received 28 November 1990; revised manuscript received 1 May 1991)

The surface-potential barrier shape for the (001) face of copper was determined by an analysis of low-energy-electron-diffraction fine-structure measurements. The fitting of the fine-structure spectra was performed with a precise knowledge of the incident diffraction conditions of the experimental data (incidence angle, azimuthal angle, and contact-potential difference). This precision is necessary to allow a consistent barrier shape to be determined. For three different angles of incidence, it was found that a good match between theoretical and experimental I-V spectra was obtained when the image plane was located 2.5 a.u. from the topmost layer of atoms.

I. INTRODUCTION

Low-energy-electron-diffraction (LEED) fine-structure features, or threshold effects, are only observed at very low energies (typically <40 eV). They arise from an interference between the measured beam (usually the specular) and another beam that has insufficient momentum perpendicular to the surface to escape the potential barrier. This preemergent beam is internally reflected at the barrier and can be rescattered by the substrate back into the direction of the measured beam. Due to the long-range image-like behavior of the barrier the resulting interference usually consists of a Rydberg-like series of peaks converging on the emergence energy of the preemergent beam. This is the energy at which the beam can escape the barrier.[1]

The structure of the threshold effects depends upon the nature of the transition of the crystal potential to the vacuum level as a function of distance from the surface. The most critical factors involved in this barrier shape are the location of the image plane for the long-range imagelike part of the potential and the saturation of this potential close to the crystal surface.[2]

In this work we have measured and analyzed LEED I-V spectra containing fine-structure effects at three different angles of incidence. These angles of incidence, the azimuthal angles, and the absolute energy scale of the spectra were known precisely by the use of an internally consistent method to determine these parameters.[3]

The theoretical LEED spectra were calculated using the transfer-matrix method of McRae[4] to find the reflectivity of a semi-infinite crystal. The method of Kambe[5] was used to include multiple scattering events. The damping within the bulk region was described by an energy-dependent imaginary component of the crystal potential as given by McRae and Caldwell,[6]

$$\mathrm{Im}U=-0.26(1+E/\phi)^{1.7}\ , \tag{1}$$

where U is the scattering potential of the crystal, E the electron energy, and ϕ the work function.

Fine-structure effects were included by the addition of a one-dimensional potential as a selvedge layer. The barrier model used was a saturated image barrier (SIB) type developed by Jones *et al.*[7] and has the form

$$V(z)=\begin{cases}\dfrac{1-\exp[\lambda(z-z_0)]}{2(z-z_0)}, & z<z_0\\ -V_0 & \\ \dfrac{}{A\exp[-B(z-z_0)]+1}, & z\geq z_0\ ,\end{cases} \tag{2}$$

where $A=-1+2V_0/\lambda$ and $B=V_0/A$. The z axis is directed into the crystal. This model has three adjustable parameters. V_0 is the inner potential of the crystal and z_0 the origin of the image part of the barrier. The degree of saturation is described by the λ parameter. It gives the value of the potential at the image plane location $[V(z_0)=-\lambda/2]$. In this work V_0 was kept constant and only z_0 and λ were varied in the calculations.

This analytic form of the barrier shape is the best currently in use and was proposed on the basis that it closely approximated the results of jellium and density functional calculations of the barrier potential.[7] It has been widely used for the fitting of both fine-structure features[2] and inverse photoemission image states.[8]

Damping within the surface region was included by specifying an imaginary part for the barrier potential. This was of the form

$$\mathrm{Im}V(z)=\mathrm{Im}U\alpha\exp(-\beta|z|),\quad z<0\ . \tag{3}$$

The parameter α indicates the magnitude of the damping and mainly affects the size of the fine-structure peaks relative to the Bragg peaks. The β parameter determines how quickly the damping dies off in vacuum and its main effect is on the relative sizes of peaks within the Rydberg-like series.

As shown by Read[9,10] it is difficult to determine unique barrier parameters from the fine-structure data. This is to be expected as the mechanism involves an interference effect and it is therefore possible to obtain relatively good fits between theory and experiment for a number of discrete barrier shapes. This simply reflects the fact that

TABLE I. Surface-potential barrier parameters for Cu(001) determined from some previous fittings of LEED fine-structure measurements using various barrier models (JSIB+IP was determined from inverse photoemission data).

Model	z_0	Saturation	V_0	Ref.
MIB	−1.3		0.8	12
MIB	−1.6		0.8	13
DSIB	−2.5	$V_1=0.5$	0.85	15
DSIB	−3.7	$V_1=0.4$	0.88	8,9
JSIB	−2.35	$\lambda=1.05$	0.85	10
JSIB+IP	−2.18	$\lambda=1.17$	1.08	11
JSIB	−2.50	$\lambda=0.90$	0.85	This work

the interference phenomenon repeats for every 2π difference in the phase. However, in our analysis we have used as a basis for our parameter space search the theoretical estimates as determined by Jennings *et al.*[11] in their density functional thin film calculations. We expect these values to provide a good indication of the "true" values.

The Cu(001) potential energy barrier shape has been studied previously, both experimentally and theoretically. Table I summarizes some of the previous fits of LEED fine structure with surface barrier models. Included in this table are the parameters determined by Smith *et al.*[8] using inverse photoemission (IP) data of image states on Cu(001).

Early work by Jennings and co-workers[12,13] used a modified image barrier (MIB) which did not allow any significant saturation of the barrier potential. The first shape determination using an SIB was by Dietz *et al.*[14] The functional form of the Dietz SIB (DSIB) included a parameter V_1. This can be loosely compared with $\lambda/2$ in the Jones *et al.*[7] SIB (JSIB) given by Eq. (2). Small values of either indicate a large degree of saturation of the potential. Most of the SIB work in Table I concentrated on one fine-structure spectrum measured by Dietz *et al.*[14] Jennings *et al.*[15] also included their own data in their analysis. In the IP fit of Smith *et al.*,[8] using the JSIB, z_0 was the only free parameter. V_0 and λ were set to the values as determined by matching the JSIB with a first principles calculation using the full-potential linearized augmented-plane-wave (FLAPW) method.

Table II lists some of the previous theoretical determinations of the surface-potential barrier shape for Cu(001). The first two tabled entries were found by Jennings *et al.*[11] by fitting the JSIB to the theoretical data of Lang and Kohn.[16] The electron density parameter for fit a was $r_s=2$ and that for fit b was $r_s=4$ (for copper $r_s=2.67$). Jennings *et al.*[11] also fitted the JSIB to their calculations of the planar averages of the total potential for a thin film of Cu(001) using the FLAPW method. The z_0 value using the jellium method was estimated from various calculations[17–20] for an r_s value equivalent to that of copper.

TABLE II. Parameters from some previous theoretical determinations of the surface-potential barrier shape of Cu(001).

Model	z_0	Saturation	V_0	Ref.
JSIB+LK[a]	−2.41	$\lambda=1.25$	1.21	10
JSIB+LK[b]	−2.35	$\lambda=0.62$	0.46	10
JSIB+LAPW	−2.40	$\lambda=1.15$	1.12	10
Jellium	−3.0			17–20

[a] $r_s=2$.
[b] $r_s=4$.

II. EXPERIMENT

The apparatus used to obtain the fine-structure data was mounted in a UHV chamber and has been described previously.[21] A 127° cylindrical deflecting analyzer (CDA) was used to monochromate electrons from a hot tungsten filament. This provided a beam with an energy resolution of 70 meV and an angular divergence of around 1°. Elastically scattered electrons were collected by a three-grid retarding field analyzer. The system was designed so that the angles of incidence and azimuth could be varied continuously.

The overall energy resolution associated with a fine-structure feature depends upon the speed of emergence of the preemergent beam causing that structure as well as the energy and angular resolution of the incident beam.[22] We have shown previously how this "equivalent resolution" varies as the incidence conditions change.[3,22] We have also shown how it is possible to unambiguously determine the angles of incidence and azimuth for these fine-structure measurements.[3]

The copper crystal was prepared using techniques described elsewhere.[23] The surface was mechanically ground and polished and then electropolished. *In situ* cleaning consisted of argon ion bombardment and annealing cycles. Surface cleanliness and order were monitored using LEED and Auger electron spectroscopy (AES).

III. RESULTS AND ANALYSIS

Figure 1 shows the match between theory and experiment for the barrier shape parameters that gave best fit over the range of incident angles shown. The calculated spectra have been convoluted with Gaussian functions to simulate experimental resolution. The half-widths of these functions corresponded to the appropriate equivalent resolution for each angle.[22]

In determining the optical parameters z_0 was varied from −1.7 to −4.2 and λ from 0.65 to 1.15 a.u. Figure 2 shows a contour plot of *r*-factor values versus the image plane position and barrier saturation for an incident angle of 63°. The *r* factor employed here is the average percentage deviation of the peak and dip positions. Similar plots were obtained for the other angles of incidence. There was an unambiguous area of best fit that gave parameters for the potential of Eq. (2) of $z_0=-2.5\pm0.1$ and $\lambda=0.90\pm0.05$. The inner potential V_0 was set at 0.85 Ry.[24] The barrier damping function parameters that best reproduced the relative peak heights of the LEED spectra were $\alpha=1$ and $\beta=0.4$. These were not extensively optimized and represent estimates only of these values.

The barrier parameters obtained in this work agree reasonably well with those obtained by Jennings *et al.*[11] using the JSIB model on the data of Dietz *et al.*[14] The

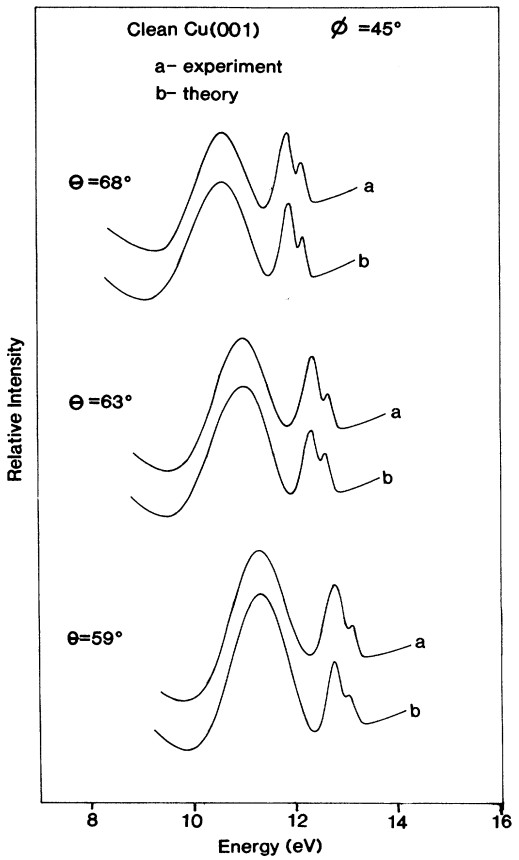

FIG. 1. Comparison between calculated (using $z_0 = -0.5, \lambda = 0.9$) and measured LEED fine structure from Cu(001) for three angles of incidence along the ⟨11⟩ azimuth. Calculated spectra have been convoluted with Gaussian functions to simulate experimental resolution.

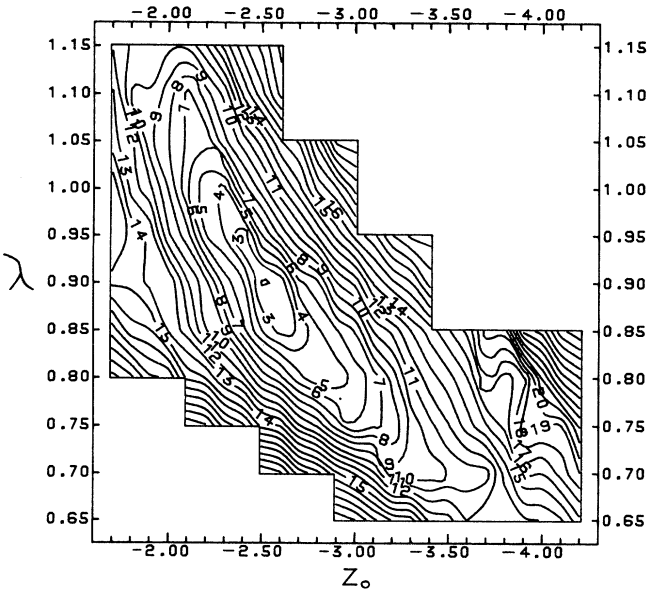

FIG. 2. Contour plot showing r-factor values (average percentage deviation of peak and dip positions) as a function of image plane position z_0 and barrier saturation λ for an incident angle of 63°.

image plane location also agrees with that obtained by Jennings *et al.*[15] using the DSIB model but differs markedly from that of Read[8,9] using the same model. The jellium value for z_0 is slightly larger than, but not substantially different from, the value obtained in this work. However, it should be noted that the z_0 parameter used in the LEED barrier models is not exactly equivalent to the z_0 in the jellium calculations. LEED experiments use moving electrons. The effective z_0 determined from such experiments will be energy dependent and lie closer to the surface than the static image plane.[25,26]

IV. DISCUSSION

The high quality of the agreement between experiment and theory gives us confidence that we can indeed determine the barrier constants on this surface. The data are self-consistent in that we have a high degree of certainty in the angles of incidence, azimuth, and contact-potential difference. The barrier parameters quoted fit over a range of angles of incidence and azimuth.

The fine-structure features from the Cu(001) surface fall at energies (near 60° incidence) where the background is relatively flat and the inelastic damping is well described by Eq. (1). Under these circumstances, the exact form of the variation in inner potential with energy and the variation in the imaginary part of the inner potential (the inelastic damping) are not important. This is not the case for instance for the W(001) surface. For this surface Baribeau *et al.*[27] concluded they were unable to find unequivocal values of the barrier parameters because of the interdependence of the damping and inner potential with the barrier parameters. We have noted similar effects for the Cu(111) surface[28] but this appears not to be the case for the Cu(001) surface.

ACKNOWLEDGMENTS

This work was partly funded by the Australian Research Council (ARC). One of us (G.J.H.) was also supported in part by the ARC.

[1]E. G. McRae, Rev. Mod. Phys. **51**, 541 (1979).
[2]R. O. Jones and P. J. Jennings, Surf. Sci. Rep. **9**, 165 (1988).
[3]G. Hitchen and S. Thurgate, Phys. Rev. B **38**, 8668 (1988).
[4]E. G. McRae, Surf. Sci. **11**, 479 (1968).
[5]K. Kambe, Z. Naturforsch. **22A**, 322 (1967); **23A**, 1280 (1968).
[6]E. G. McRae and C. W. Caldwell, Surf. Sci. **57**, 766 (1976).
[7]R. O. Jones, P. J. Jennings, and O. Jepsen, Phys. Rev. B **29**, 6474 (1984).

[8]N. V. Smith, C. T. Chen, and M. Weinert, Phys. Rev. B **40**, 7565 (1989).
[9]M. N. Read, Phys. Rev. B **32**, 2677 (1985).
[10]M. N. Read, Appl. Surf. Sci. **22/23**, 48 (1985).
[11]P. J. Jennings, R. O. Jones, and M. Weinert, Phys. Rev. B **37**, 6133 (1988).
[12]G. L. Price, P. J. Jennings, P. E. Best, and J. C. L. Cornish, Surf. Sci. **89**, 151 (1979).
[13]P. J. Jennings and G. L. Price, Surf. Sci. **93**, L124 (1980).
[14]R. E. Dietz, E. G. McRae, and R. L. Campbell, Phys. Rev. Lett. **45**, 1280 (1980).
[15]P. J. Jennings, S. M. Thurgate, and G. L. Price, Appl. Surf. Sci. **13**, 180 (1982).
[16]N. D. Lang and W. Kohn, Phys. Rev. B **1**, 4555 (1970).
[17]N. D. Lang and W. Kohn, Phys. Rev. B **7**, 3541 (1973).
[18]P. A. Serena, J. M. Soler, and N. Garcia, Phys. Rev. B **34**, 6767 (1986).
[19]S. Ossicini, F. Finocchi, and C. M. Bertoni, Surf. Sci. **189/190**, 776 (1987).
[20]A. Liebsch, Phys. Rev. B **32**, 6255 (1985).
[21]S. Thurgate and G. Hitchen, Appl. Surf. Sci. **24**, 202 (1985).
[22]G. Hitchen and S. Thurgate, Surf. Sci. **197**, 24 (1988).
[23]S. M. Thurgate and P. J. Jennings, Surf. Sci. **114**, 395 (1982).
[24]P. J. Jennings and S. M. Thurgate, Surf. Sci. **104**, L210 (1981).
[25]E. Zaremba and W. Kohn, Phys. Rev. B **13**, 2270 (1976).
[26]A. Liebsch, Phys. Rev. B **33**, 7249 (1986).
[27]J. M. Baribeau, J. D. Carette, P. J. Jennings, and R. O. Jones, Phys. Rev. B **32**, 6131 (1985).
[28]G. J. Hitchen and S. M. Thurgate (unpublished).